https://doi.org/10.5194/egusphere-2024-423
Preprint. Discussion started: 26 February 2024

Effect of the 2022 summer drought across forest types in Europe

Mana Gharun[1], Ankit Shekhar[2], Jingfeng Xiao[3], Xing Li[4], Nina Buchmann[2]

[1]Institute of Landscape Ecology, University of Münster, Germany
[2] Institute of Agricultural Sciences, ETH Zürich, Switzerland
[3] Earth Systems Research Center, University of New Hampshire, USA
[4] Research Institute of Agriculture and Life Sciences, Seoul National University, South Korea

Correspondence to: Mana Gharun, mana.gharun@uni-muenster.de

Abstract

Forests in Europe experienced record-breaking dry conditions during the 2022 summer. The direction in which various forest types respond to climate extremes during their growing season is contingent upon an array of internal and external factors. These factors include the extent and severity of the extreme conditions and the tree ecophysiological characteristics adapted to environmental cues, which exhibit significant regional variations. In this study we aimed to: 1) quantify the extent and severity of the extreme soil and atmospheric dryness in 2022 in comparison to two most extreme years in the past (i.e., 2003, 2018), 2) quantify response of different forest types to atmospheric and soil drought in terms of canopy browning and photosynthesis, and 3) relate the functional characteristics of the forests to the emerging responses observed at the canopy level. For this purpose, we used the ERA5-Land spatial meteorological dataset between 1970 to 2022 to identify conditions with extreme soil and atmospheric dryness. We used the near-infrared reflectance of vegetation (NIRv) derived from the MOderate Resolution Imaging Spectroradiometer (MODIS), and the OCO-2 solar induced fluorescence (SIF) as an observational proxy for photosynthesis based on the SIF data product, to quantify the response of forests at the canopy level.

In summer 2022, particularly southern regions of Europe experienced the most pronounced atmospheric and soil dryness. As a result, the extremely dry conditions led to an average 30% more widespread decline in SIF across forests compared to drought

https://doi.org/10.5194/egusphere-2024-423
Preprint. Discussion started: 26 February 2024

in 2018, and 60% more widespread decline compared to drought in 2003. Although the atmospheric and soil drought were more extensive and severe (indicated by a larger observed max z-score) in 2018 compared to 2022, the negative impact on forests, indicated by declined SIF, was significantly larger in 2022. Across different forest types, the deciduous broad-leaved forests were most negatively affected by the extreme conditions in 2022, but Evergreen Needle-Leaf Forests (ENF) distributed in northern regions of Europe showed enhanced canopy greening and SIF signals as a benefit of warming. Higher degree of canopy damage in 2022 in spite of less extreme conditions compared to the previous extreme year points to a legacy effect on forest canopies, and a declined forest resilience in response to more frequent drought events.

Keywords: *photosynthesis, soil drought, atmospheric drought, canopy browning, gross primary production*

Introduction

The frequency and intensity of drought events have been increasing globally, and future global warming will continue to increase the occurrence of such events (Seneviratne et al. 2012; Röthlisberger and Papritz 2023). Particularly over the past two decades, over many regions in Europe, there have been reports of widespread drought conditions, for example during the summers of 2003, 2010 and 2018 (Bastos et al. 2020; Zhou et al. 2023). Such extreme conditions lead to widespread ecological disturbance (Müller and Bahn 2022) and reduced capacity of forests for carbon uptake which diminishes their potential for mitigating climate change (van der Woude et al. 2023). Additionally, heatwave and prolonged drought periods stress vegetation and increase their susceptibility to other biotic and abiotic stress factors, increase tree mortality and risk of wildfire, lead to loss of biodiversity of plants and animals that live on the edge of their temperature tolerance, and change phenology and plant development with cascading effects on the functioning of the ecosystem (Seidl et al. 2017).

The spatial extent and severity of drought events vary, and the impacts depend on the local ecological characteristics of the forests, species-specific temperature and moisture

https://doi.org/10.5194/egusphere-2024-423
Preprint. Discussion started: 26 February 2024

threshold that limit tree functioning, and adaptation strategies and acclimation of trees to more frequent and more intense extreme conditions (Gessler et al. 2020). For example, comparing the 2003 and 2018 extreme years, the year 2018 was characterized by a climatic dipole, featuring extremely hot and dry weather conditions north of the Alps but comparably cool and moist conditions across large parts of the Mediterranean. Negative drought impacts appeared to affect an area 1.5 times larger and to be significantly stronger in summer 2018 compared to summer 2003 (Buras et al. 2020).

In 2022 Europe experienced its second hottest and driest year on record and the summer of 2022 was the warmest summer ever recorded. Conditions in summer 2022 led to record-breaking heatwave and drought events across many regions (Copernicus Climate Change Service, 2023). Compound drought and heatwave conditions in 2022 caused widespread crop damage, water shortages, and wildfires across Europe. The hardest-hit areas were Iberian Peninsula, France, and Italy, where temperatures exceeded 2.5°C above normal, and severe droughts persisted from May to August (Tripathy and Mishra 2023). The reduced soil moisture due to precipitation deficits and high temperatures, contributed to the persistence and severity of drought, creating a positive feedback loop where dry soils led to even drier conditions (Tripathy and Mishra 2023).

Drought and heatwaves have diverse negative impacts on the functioning of trees and forests. The most immediate response is that rising air temperature and increased dryness (in the soil or in the atmosphere) leads to changes in mesophyll and stomatal conductance that affect carbon uptake (Marchin et al. 2021). Plants reduce stomatal conductance under severe drought to reduce water stress at the expense of reduced rates of photosynthesis (Oren et al., 1999). Drought also increases the chance of hydraulic failure and leads to tree mortality (Choat et al. 2018). In addition, under rising temperatures enzymatic activity of trees is reduced which also decreases the gross primary productivity of the forest (Gourlez de la Motte et al. 2020). Elevated temperatures can also increase rates of respiration from the soil and from the trees which leads to reduced net capacity of forests for carbon uptake and reducing anthropogenic CO_2 emissions (van der Molen et al. 2011; Anjileli et al. 2021). Drought also limits movement of nutrients in the soil water and decreases nutrient availability to trees which would affect growth and productivity (Bauke et al. 2022).

https://doi.org/10.5194/egusphere-2024-423
Preprint. Discussion started: 26 February 2024

Changes in plant water-use and nutrient cycling can trigger feedback loops that magnify the effects of drought and heat stress. For instance, reduced plant cover can increase soil temperatures and further accelerate water loss and increase plant water demand (Haesen et al. 2023). On the other hand, increased atmospheric dryness or reduced soil moisture levels increase stomatal closure which limits transpiration and leads to higher leaf temperature that intensifies heat stress on plants (Drake et al. 2018). Reduced transpiration and photosynthesis lead to increased surface temperature and CO_2 concentration in the atmosphere, both of which change local and regional climate patterns and accelerate the frequency and intensity of extreme events (Humphrey et al. 2018). These responses depend largely on forest type and species composition, which combined with the properties of the extreme (in terms of extent and severity) complicates our understanding of how drought influences the functionality of different forest ecosystems (Gharun et al. 2020; Shekhar et al. 2023a). These feedback loops underscore the critical need to evaluate the repercussions of climate extremes on different forest types, which play a pivotal role in sequestering significant portions of anthropogenic emissions from the atmosphere, under a drying climate. Our objectives in this study are thus to 1) quantify the extent and severity of the extreme conditions in 2022 (in terms of soil and atmospheric dryness) and compare that to two past extreme years (i.e., 2003, 2018), 2) quantify response of different forest types to drought in terms of canopy browning and photosynthesis, and 3) relate the functional characteristics of the forests to the emerging responses observed at the canopy level.

Methods

Meteorological dataset

We used Europe-wide (Longitude: 11°W - 32°E; Latitude: 35.8°N -72°N, approximate area of 4.45 million km^2) gridded datasets of daily total precipitation (Precip; mm), daily mean air temperature (Tair; °C), daily mean relative humidity (RH; %) and daily mean soil moisture (SM; m^3m^{-3}) of topsoil layer (0-7 cm depth), spanning from 2000-2022. We obtained the Precip, Tair and RH datasets from the E-OBS v27.0e dataset (daily at

https://doi.org/10.5194/egusphere-2024-423
Preprint. Discussion started: 26 February 2024

0.1°×0.1° resolution; Cornes et al., 2018; Klein et al., 2002), and SM was extracted from the most recent reanalysis data from ECMWF's (European Centre for Medium-range Weather Forecasts), new land component of the fifth generation of European Reanalysis (ERA5-Land) dataset (daily at 0.1°×0.1° resolution; Munoz-Sabater et al., 2021). We calculated vapor pressure deficit (VPD; kPa) from Tair and RH using Equation 1.

$$VPD = (1 - \frac{RH}{100}) \times 0.6107 \times 10^{\frac{7.5 \times Tair}{237.3 + Tair}} \quad (1)$$

We re-sampled the Precip, Tair, VPD, and SM values from daily (at 0.1°×0.1°) to 8-day (at 0.05°×0.05°) to match the temporal and spatial resolution of vegetation response dataset (see next section).

Forest canopy response dataset

In order to assess the forest canopy response to drought stress, we used two satellite-based proxies: 1) the structure-based NIRv (near-infrared of vegetation index derived from MODIS (Moderate Resolution Imaging Spectroradiometer)(Equation 2), and 2) the physiological-based reconstructed global OCO-2 solar induced fluorescence (SIF). NIRv was estimated following Badgley et al. (2017) as:

$$NIR_V = R_{NIR} \times \frac{R_{NIR} - R_{Red}}{R_{NIR} + R_{Red}} \quad (2)$$

where, R_{NIR} and R_{Red} are the surface spectral reflectance at near-infrared band (band 2 of MODIS) and reflectance at red band (band 1 of MODIS), respectively. We obtained the R_{NIR} and R_{Red} from MODIS MOD09Q1 v6.1 product which provides R_{NIR} and R_{Red} at a 8-day temporal and 500m spatial resolution. The calculated NIRv at 500m resolution was aggregated (by mean) at a 0.05°×0.05° resolution. Solar-induced fluorescence (SIF) is

https://doi.org/10.5194/egusphere-2024-423
Preprint. Discussion started: 26 February 2024

linked to vegetation photosynthesis and can be used as a proxy for the ecosystem's gross primary productivity (GPP) (Li et al. 2018; Magney et al. 2019). SIF was available from 2000-2022 at 8-day temporal scale with a spatial resolution of 0.05°×0.05° (Li and Xiao, 2019). SIF signals provide information about physiological response of forest photosynthesis while NIRv (a recently developed vegetation index) signals provide information about the health status of the canopy. NIRv is preferred over NDVI and EVI as it can isolate the vegetated signal, mitigate mixed-pixel issue, and partly address the influences of background brightness and soil contamination (Zhang et al. 2022). The two indices are expected to provide complementary information on vegetation functions.

Land cover dataset

In this study we focused on five different types of forests (and woodlands) across Europe, namely, evergreen needleleaf forest (ENF), evergreen broadleaf forest (EBF), deciduous broadleaf forest (DBF), mixed forest (MF), and woody savannas (WSA). The spatial distribution of the five different forest types across Europe is shown in Figure 1. We used the yearly MODIS land cover product (MCD12C1 version 6.1 at 0.05°×0.05° resolution) for the years of 2001, 2006, 2011, 2016 and 2021, to extract total areas covered by each forest type. Only areas that were consistently identified as each forest type in those five years were included in the analysis. This means that only pixels common across the selected five years were selected (Supplementary Fig. 1), and with more than 50% of the 0.05°×0.05° pixel area identified as forests (Supplementary Fig. 1). The selected forested area in this study covered an area of 907´875 km^2 (about 24% of total land area of Europe) (Figure S1). Out of the total area about 23% (206´212 km^2) was dominated by ENFs

https://doi.org/10.5194/egusphere-2024-423
Preprint. Discussion started: 26 February 2024

distributed largely across Northern Europe (NEU). Approximately 1% (7´000 km^2) of the area was dominated by EBFs, located entirely in Mediterranean Europe (MED), and about 10% (92´209 km^2) was dominated by DBF which was largely distributed across MED. Approximately 20% (174´934 km^2) of the total forested area was dominated by MFs largely dominating Central Europe (CEU), and about 47% (427´529 km^2) was dominated by WSA mostly found in NEU (Figure 1).

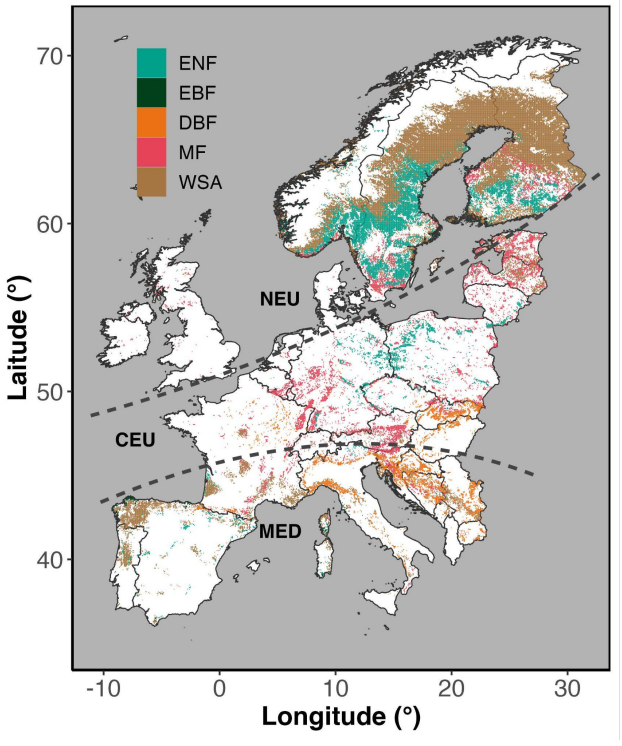

Figure 1 Spatial coverage of forests (ENF - evergreen needleleaf forest; EBF - evergreen broadleaf forest; DBF - deciduous broadleaf forest; MF - mixed forest), and woodlands (WSA - woody savannas) across Europe, after selection (see methods). Areas are differentiated into Northern Europe (NEU), Central Europe (CEU), and Mediterranean Europe (MED) following Markonis et al. (2021). The map is based on MODIS land cover product MCD12C1 (version 6.1).

https://doi.org/10.5194/egusphere-2024-423
Preprint. Discussion started: 26 February 2024

Statistical data analysis

The focus of our analysis was on the summer months during three extreme years of 2003, 2018 and 2022. For this purpose, we subset our meteorological (Precip, Tair, and VPD), soil moisture (SM), and vegetation proxy (NIRv and SIF) datasets for the months of June, July, August (JJA) which comprised of fourteen 8-day periods, for each forested pixel between 2000 and 2022.

In order to exclude any impact of the observed greening trend across Europe on the anomalies of vegetation proxies during the extreme years (2003, 2018, 2022), we used detrended summer mean NIRv and SIF. Detrending of summer mean NIRv and SIF from 2000-2022 was done pixel-wise based on a simple linear regression model (Buras et al., 2020). We calculated pixel-wise standardized summer anomalies (in terms of z-score, Var_z) for all the variables (Var), i.e., Precip, Tair, VPD, SM, NIRv, and SIF, for each extreme year using Equation 3. Z-scores less than -1 and more than 1 indicate significant negative and significant positive anomalies beyond normal variability. Var_z is calculated as:

$$Var_z\ (unitless) = \frac{Var - Var_{mean}}{Var_{sd}} \quad (3)$$

where, Var_{mean} and Var_{sd} are mean and standard deviation of any variable over the 2000-2022 period. Areas were categorized as under drought if $VPD_z > 1$ & $SM_z < -1$, and as normal areas if $-1 < VPD_z < 1$ & $-1 < SM_z < 1$. We used the Pearson correlation coefficient (r) and partial correlation coefficients (Pr) to understand the spatial (across space for each year) and temporal (during each year) correlation of SIF and NIR_v anomalies with SM and VPD anomalies (Dang et al., 2022). We calculated the partial correlation coefficient using equations 4-7:

$$Pr(SIF,SM) = \frac{r(SIF,SM) - r(SIF,VPD)\times r(SM,VPD)}{\sqrt{1-r(SIF,VPD)^2} - \sqrt{1-r(SM,VPD)^2}} \quad (4)$$

$$Pr(SIF,VPD) = \frac{r(SIF,VPD) - r(SIF,SM)\times r(SM,VPD)}{\sqrt{1-r(SIF,SM)^2} - \sqrt{1-r(SM,VPD)^2}} \quad (5)$$

https://doi.org/10.5194/egusphere-2024-423
Preprint. Discussion started: 26 February 2024

$$Pr(NIRv,SM) = \frac{r(NIRv,SM) - r(NIRv,VPD) \times r(SM,VPD)}{\sqrt{1-r(NIRv,VPD)^2} - \sqrt{1-r(SM,VPD)^2}} \quad (6)$$

$$Pr(NIRv,VPD) = \frac{r(NIRv,VPD) - r(SIF,SM) \times r(SM,VPD)}{\sqrt{1-r(NIRv,SM)^2} - \sqrt{1-r(SM,VPD)^2}} \quad (7)$$

Results

Severity of the 2022 summer drought compared to 2018 and 2003

Figure 2 shows the extent and magnitude of anomalies (z-score) of VPD and top layer (0-7 cm) soil moisture content during the summer months in 2003, 2018, and 2022 across the entire region of Europe. In summer 2022, particularly southern regions of Europe experienced the most pronounced increase in atmospheric (z-score > 1) and soil dryness (z-score < -1) (Figure 2) while in 2018 we observed the most widespread drought in northern Europe (Figure 2).

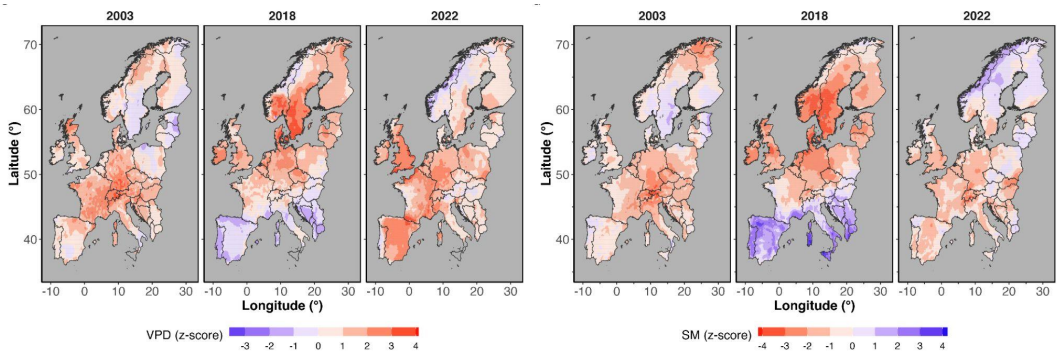

Figure 2 Standardized summer (JJA) anomalies (z-score) of mean vapor pressure deficit (VPD), and top layer (1-7 cm depth) soil moisture (SM) in 2003, 2018 and 2022, across the region of Europe.

Restricted to forested areas, atmospheric and soil drought was 55% and 58% more extensive in 2018 compared to 2022 (and both years more extensive than in 2003, Figure 3). In 2022, 28 Mha of forested areas in Europe experienced an extremely high VPD (z-score > 1), while in 2018 63 Mha experienced such extreme conditions. In 2022, 21 Mha

https://doi.org/10.5194/egusphere-2024-423
Preprint. Discussion started: 26 February 2024

of forested areas experienced an extremely low soil moisture content (z-score < -1) while in 2018, 50 Mha of forests in Europe were affected by such extreme conditions. In 2003 an area of 25 Mha was affected by extremely dry air and a similar area was affected by extremely dry soil (Figure 3).

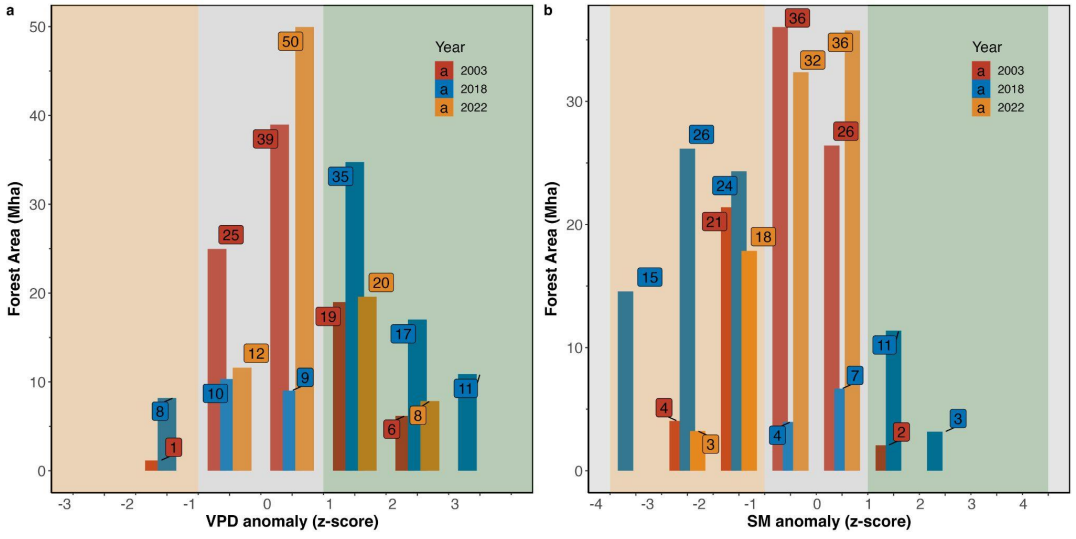

Figure 3 Intensity (z-score) and extent (area affected, Mha) of (a) VPD, and (b) SM anomalies across forested areas. Z-score, values from -1 and 1 are considered normal (within 1 standard deviation of the mean).

Forest canopy response to the 2022 drought

Compared to 2018, the extremely dry conditions in 2022 led to 30% increase in forested areas that exhibited declined photosynthesis (17 Mha in 2022 compared to 12 Mha in 2018) (Figure 4). The extent of the canopy browning observed in 2022 was similar to 2018, which in both years was 120% of the extent of observed canopy browning in 2003 (11 Mha compared to 5 Mha observed in 2003) (Figure 4).

https://doi.org/10.5194/egusphere-2024-423
Preprint. Discussion started: 26 February 2024

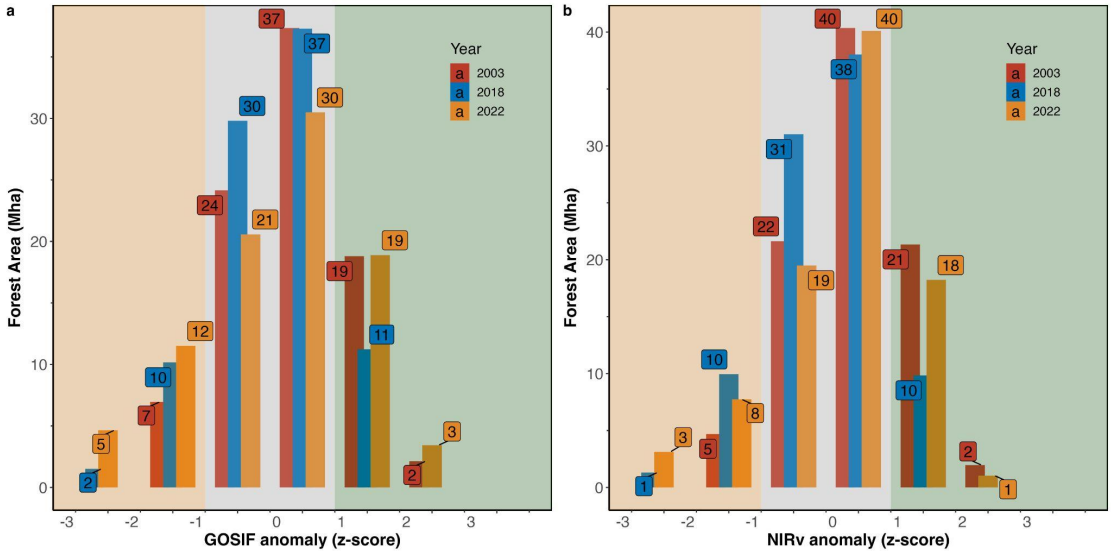

Figure 4 Intensity (z-score) and extent (area affected, Mha) for (a) SIF, and (b) NIRv anomalies across forested areas. Z-score, values from -1 and 1 are considered normal (within 1 standard deviation of the mean).

Across specific forest types, DBFs showed the largest negative SIF anomaly in 2022 but the ENFs showed a positive SIF anomaly in 2022, both in terms of magnitude and in terms of the spatial extent of negative SIF anomalies (Figure 5). In terms of canopy browning response (NIRv anomalies), the largest negative NIRv anomalies in 2022 were observed in southern Europe (Figure 6). Largest negative NIRv anomalies (indicated by the maximum anomaly) were observed in the DBFs in 2022, fitting the declined SIF signals. The ENFs however showed positive NIRv anomalies in 2022, also both in terms of magnitude and spatial coverage and % of total area affected (Figure 6).

https://doi.org/10.5194/egusphere-2024-423
Preprint. Discussion started: 26 February 2024

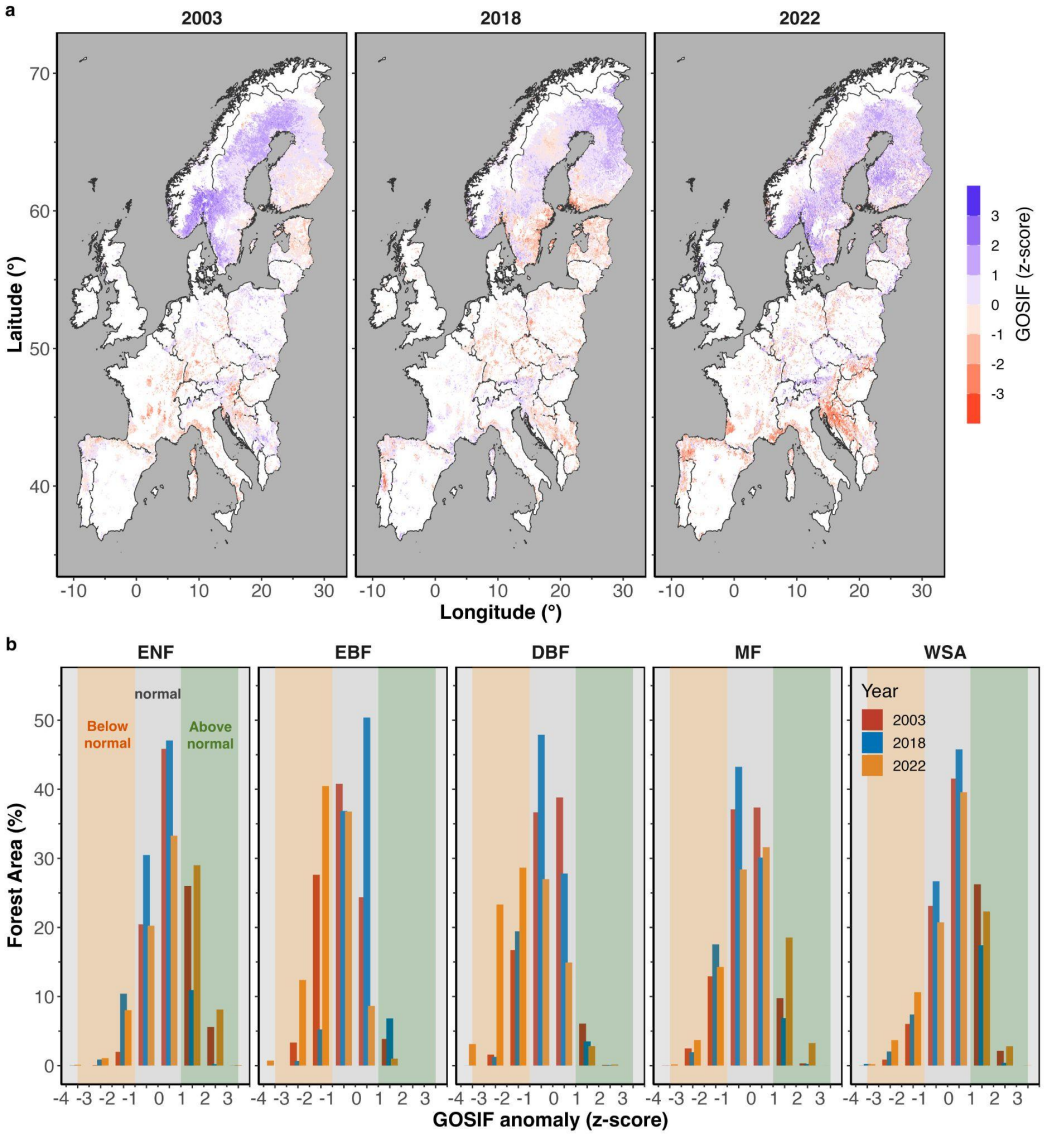

Figure 5 (a) SIF anomaly (in terms of z-score) across Europe, and (b) area coverage (in terms of percentage of total area for each forest type) in 2003, 2018 and 2022.

https://doi.org/10.5194/egusphere-2024-423
Preprint. Discussion started: 26 February 2024

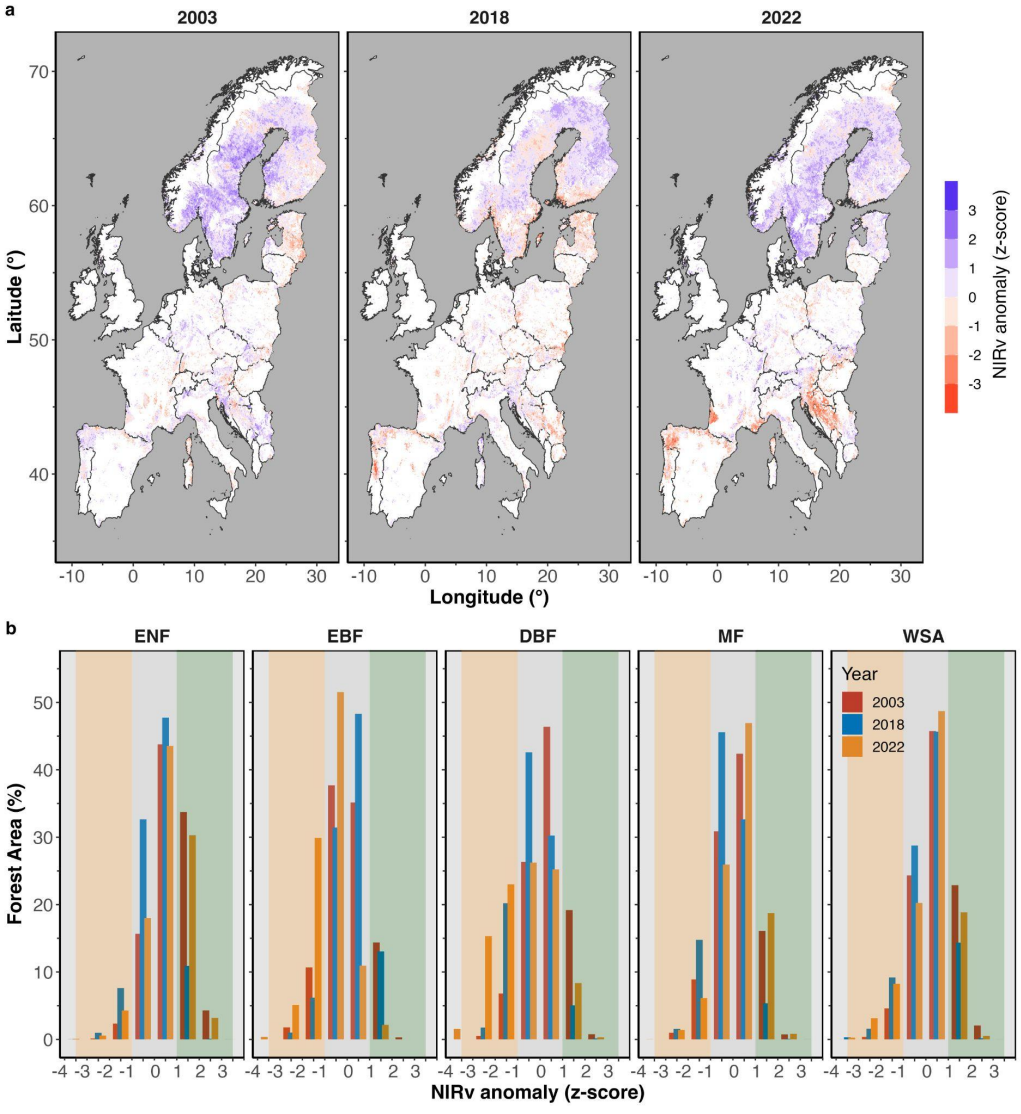

Figure 6 (a) NIRv anomaly (in terms of z-score) across Europe, and (b) area coverage (in terms of percentage of total area for each forest type) in 2003, 2018 and 2022.

Relationship between SIF and NIRv

In general, the values of NIRv and SIF were highly correlated (Supplementary Figure 1). The anomalies in NIRv and SIF were most correlated across WSAs (mean r^2 = 0.62) and least correlated across the ENFs (Supplementary Figure 1). With the increase in VPD

https://doi.org/10.5194/egusphere-2024-423
Preprint. Discussion started: 26 February 2024

273 positive anomalies (i.e., increased atmospheric dryness), SIF values declined across all
274 forest types, across all years, except in 2022 in the WSA, and in 2018 and 2022 in EBFs
275 (Figure 7). With decrease in soil moisture (i.e., increased soil dryness), SIF values also
276 declined overall (r^2 = 34), but not as strongly as with the increase in air dryness (r^2 = 39)
277 (Figure 7). Across different forest types, SIF responded most strongly to VPD anomalies
278 in the MFs (mean r^2 = 0.48), and responded most directly to changes in the soil moisture
279 in the WSA (Figure 7).

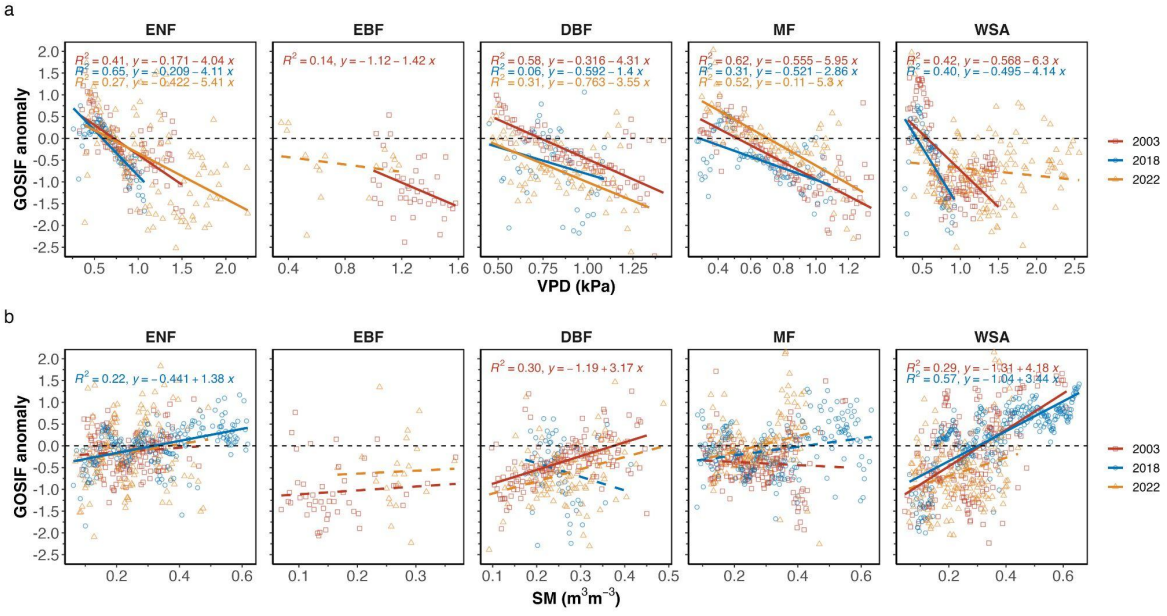

280
281 **Figure 7** Spatial regression between standardized SIF anomalies with (a) VPD and (b) SM over
282 the drought areas in summers 2003, 2018 and 2022. Dashed lines mark an insignificant
283 relationship (p > 0.05).
284
285 Between VPD and SM, in general SIF anomalies were more correlated with VPD than
286 with SM anomalies, and the decline in VPD correlated well with the larger SIF decline that
287 we observed in DBFs in 2022 and in ENFs in 2003 (Figure 7). Under general conditions
288 (regardless of drought), response of SIF to both air dryness and soil moisture anomalies
289 were larger than the response of NIRv (r^2 = 0.39 with SIF, compared to r^2 = 0.29 for NIRv)
290 (Figure 7, 8).

https://doi.org/10.5194/egusphere-2024-423
Preprint. Discussion started: 26 February 2024

The SM and VPD anomalies across all forest types correlated well, but across DBFs the dryness in the atmosphere and the dryness in the soil were most correlated (Figure 9). In terms of canopy response to VPD, ENF were the forests that responded most strongly to changes in the atmospheric dryness (Figure 9).

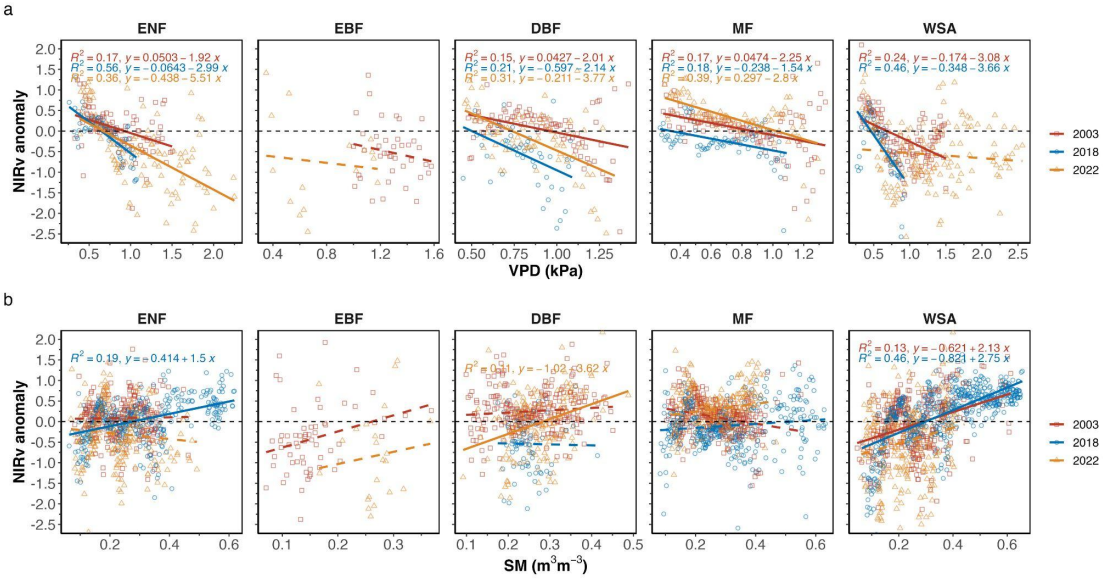

Figure 8. Spatial (over all pixels) regression between standardized NIRv anomalies with (a) VPD and (b) SM over the drought areas and normal areas in 2003, 2018 and 2022.

https://doi.org/10.5194/egusphere-2024-423
Preprint. Discussion started: 26 February 2024

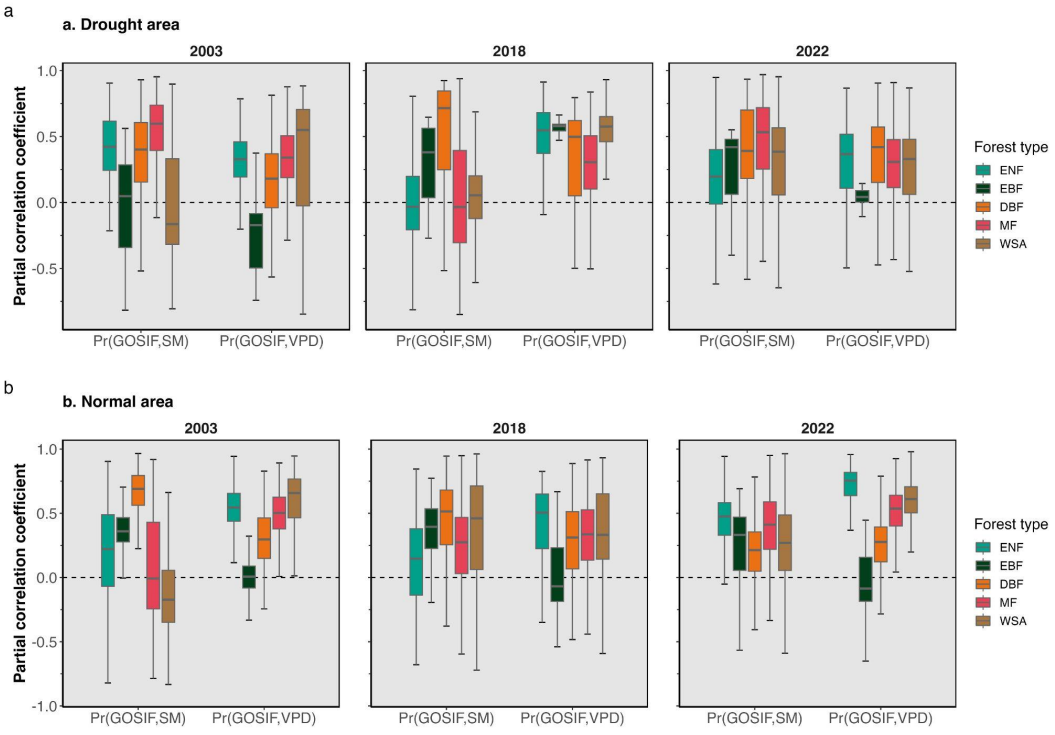

Figure 9. Temporal partial correlation coefficient of SIF with SM and VPD during summer for detected (a) drought areas and (b) normal areas. A similar figure for NIRv is Supplementary Figure 2.

Discussion

Severity of the 2022 summer drought

While the three selected years (2003, 2018, 2022) are all characterized as "extreme" years, characteristics of the extreme conditions varied largely across the years. In 2003 for example, the widespread negative anomalies in soil moisture indicated a significant soil drought, while in 2022 widespread larger positive VPD anomalies, signaled a drier atmosphere (Figure 3). The widespread summer drought in 2022 affected mainly regions of southern Europe, as opposed to the 2003 summer drought that affected central Europe, or the 2018 summer drought that affected central and northern Europe (Figure 2) (Bastos et al. 2020). As a result, the extremely dry conditions in 2022 led to an average

https://doi.org/10.5194/egusphere-2024-423
Preprint. Discussion started: 26 February 2024

315 30% more widespread decline in SIF across forests, compared to 2018, and a 60% more
316 widespread decline compared to 2003 (Figure 4).
317 The above-normal drier conditions during the summer compromised the photosynthetic
318 capacity of plants, and with that the capacity of the ecosystem for carbon uptake from the
319 atmosphere (Peters et al. 2018; van der Woude et al. 2023). Although the atmospheric
320 and soil drought were more extensive and severe (indicated by max observed z-score) in
321 2018 compared to 2022, the negative impact on forests, indicated by declined SIF, was
322 larger in 2022 pointing to a decreased resilience of forests to drought since previous
323 conditions in 2018.

324 *Canopy response to soil versus atmospheric dryness*
325 SIF products prove to be a reliable proxy for vegetation gross productivity, as comparison
326 with ground-based flux measurements show (Shekhar et al. 2022; Pickering et al. 2022).
327 NIRv and SIF signals correspond well and are known to present seasonal patterns in
328 GPP well (Getachew Mengistu et al. 2021). While the strength of their relationship varies
329 across time and space, and with changes in the forest type (Supplementary Figure 1),
330 reductions in SIF signals can be directly linked to reduced photosynthesis. While both SIF
331 and NIRv are good indicators of canopy response to extreme climate, SIF reflects a better
332 effect of short-term changes in the climate (Figure 7).
333 Our analysis showed that across different regions, SIF anomalies corresponded more
334 strongly to increased atmospheric dryness than to increased soil dryness (Figure 7). This
335 fits the notion that for trees, vapor pressure deficit plays a larger role in controlling the SIF
336 signals than soil moisture over shorter time scales (Pickering et al. 2022). Over shorter
337 time frames, soil moisture deficit can be mitigated by various mechanisms within the
338 rooting zone and through plant´s access to deeper sources of water, whereas no such
339 buffer exists for the impact of atmospheric dryness on tree canopies. Ground-based
340 observations in forest ecosystems (e.g., based on ecosystem or tree-level
341 measurements) have shown that atmospheric dryness can impose constraints on canopy
342 gas exchange, even when soil moisture is not within a limiting range (Gharun et al. 2014,
343 Fu et al. 2022, Shekhar et al. 2024). These findings emphasize the significance of
344 considering atmospheric dryness in limiting tree photosynthesis during extremely dry

https://doi.org/10.5194/egusphere-2024-423
Preprint. Discussion started: 26 February 2024

conditions, and demonstrate the fast response of a range of canopy types to increased levels of environmental dryness.

Canopy response to drought across different forest types

The spread of drought, as the total sum of areas across z-scores, exhibited different patterns in different years, leading to varied responses of different forest types to the climatic anomalies. Impact of drought on forests can vary largely depending on the forest type, tree species, and factors that are controlled by species composition, and past exposure to extreme conditions (Arthur and Dech 2016; Chen et al. 2022). Our analysis showed that conditions in summer 2022 reduced vegetation functioning across DBFs the most, as it was indicated by declined SIF signals (Figure 5). While deciduous broad-leaved forests were most negatively affected by the extreme conditions in 2022, Evergreen Needle-Leaf Forests (ENF) distributed in northern regions of Europe showed enhanced canopy greening and SIF signals, through benefiting from the episodic warming (Forzieri et al. 2022). The mechanisms to cope with the level of drought stress, vary largely among forest types, and depend on a combination of characteristics that control water loss through the coordination of stomatal regulation, hydraulic architecture, and root characteristics (e.g., rooting perth, root distribution, root morphology) (Gharun et al. 2020; Peters et al. 2023). Stomata of trees exhibit a high sensitivity to VPD fluctuations, causing a reduction in stomatal conductance as VPD increases, which, in turn, limits the exchange of CO_2 with the atmosphere during photosynthesis (Bonal and Guehl in 2011; Li et al. 2023). Tree species exhibit varying degrees of sensitivity in their stomatal regulation response to increasing atmospheric dryness (Oren et al. 1999). For instance, ring-porous species tend to maintain robust gas exchange even under dry conditions, in contrast to diffuse-porous species like evergreen needle-leaf forests (ENFs), which adopt a stronger stomatal regulation, reducing stomatal conductance as water availability becomes more limited (Klein 2014). This variance places plants on a spectrum of drought tolerance (Klein 2014), representing their specific water relations strategy and leads to different responses of forests within similar climate regions.

Increased frequency of extremes and declined resilience of forests

https://doi.org/10.5194/egusphere-2024-423
Preprint. Discussion started: 26 February 2024

Higher degree of canopy damage that we observed in 2022, despite less severe conditions compared to the previous extreme year, points towards a lasting impact on forest canopies—a sign of decreased forest resilience in the face of more frequent drought events (Forzieri et al. 2022). The observed decline in forest resilience indicates possible significant implications for vital ecosystem services, including forest capacity for mitigating climate change. Consequently, there is an increasing urgency to consider these trends when formulating robust forest-based mitigation strategies. This is particularly critical as future projections indicate that the frequency and intensity of extreme dryness will continue to increase across Europe by more than 3-fold by the end of the 21st century (Shekhar et al. 2023b). In this context, it becomes increasingly important to investigate the vulnerability of forests to external perturbations, and to base the mitigation of drought legacy effects on management strategies that are tailored to site-specific ecophysiological and environmental factors that control the resilience of forests to drought (McDowell et al. 2020; Wang et al. 2023; Shekhar et al. 2024).

Conclusion

The severity of the 2022 summer drought, characterized by increased atmospheric dryness, significantly compromised the photosynthetic capacity of trees, leading to widespread declines in vegetation functioning, particularly evident in deciduous broad-leaved forests. Our findings highlight the importance of considering atmospheric dryness as a critical factor influencing canopy responses during extreme climatic events, alongside soil moisture deficit. Despite less severe overall conditions compared to previous extreme years, the observed higher degree of canopy damage in 2022 suggests a declining resilience of forests to drought, raising concerns about the future climate mitigation capacity of forest ecosystems, as projections indicate a continued increase in the frequency and intensity of extreme dryness across Europe.

Competing interests

Mana Gharun is a guest editor of the Special Issue and the authors also have no other competing interests to declare

https://doi.org/10.5194/egusphere-2024-423
Preprint. Discussion started: 26 February 2024

Acknowledgements

AS acknowledges funding from the SNF funded project EcoDrive (IZCOZ0_198094).

https://doi.org/10.5194/egusphere-2024-423
Preprint. Discussion started: 26 February 2024

References

Anjileli, H., Huning, L.S., Moftakhari, H. et al. (2021) Extreme heat events heighten soil respiration. Sci Rep 11, 6632. https://doi.org/10.1038/s41598-021-85764-8

Arthur CM, Dech JP (2016) Species composition determines resistance to drought in dry forests of the Great Lakes - St. Lawrence forest region of central Ontario. Journal of Vegetation Science 27, 914-925.

Badgley G et al. (2017) Canopy near-infrared reflectance and terrestrial photosynthesis.Sci. Adv.3,e1602244.DOI:10.1126/sciadv.1602244

Bastos A et al. (2020) Impacts of extreme summers on European ecosystems: a comparative analysis of 2003, 2010 and 2018. Phil. Trans. R. Soc. B 375: 20190507. http://dx.doi.org/10.1098/rstb.2019.0507

Bauke, S. L., Amelung, W., Bol, R., Brandt, L., Brüggemann, N., Kandeler, E., Meyer, N., Or, D., Schnepf, A., Schloter, M., Schulz, S., Siebers, N., von Sperber, C., & Vereecken, H. (2022). Soil water status shapes nutrient cycling in agroecosystems from micrometer to landscape scales. Journal of Plant Nutrition and Soil Science, 185, 773–792. https://doi.org/10.1002/jpln.202200357

Bonal, D. & Guehl, J.-M. (2011) Contrasting patterns of leaf water potential and gas exchange responses to drought in seedlings of tropical rainforest species. Functional Ecology, 15, 490–496.

Buras, A., Rammig, A., and Zang, C. S. (2020) Quantifying impacts of the 2018 drought on European ecosystems in comparison to 2003, Biogeosciences, 17, 1655–1672, https://doi.org/10.5194/bg-17-1655-2020.

Chen, Y., Vogel, A., Wagg, C. et al. (2022) Drought-exposure history increases complementarity between plant species in response to a subsequent drought. *Nat Commun* 13, 3217. https://doi.org/10.1038/s41467-022-30954-9

Choat, B., Brodribb, T.J., Brodersen, C.R. et al. (2018) Triggers of tree mortality under drought. Nature 558, 531–539. https://doi.org/10.1038/s41586-018-0240-x

https://doi.org/10.5194/egusphere-2024-423
Preprint. Discussion started: 26 February 2024

435 Cornes, R. C., van der Schrier, G., van den Besselaar, E. J. M., & Jones, P. D. (2018). An
436 Ensemble Version of the E-OBS Temperature and Precipitation Data Sets. Journal of
437 Geophysical Research: Atmospheres, 123(17), 9391–9409.
438 https://doi.org/10.1029/2017JD028200

439 Dang, C., Shao, Z., Huang, X., Qian, J., Cheng, G., Ding, Q., & Fan, Y. (2022). Assessment of
440 the importance of increasing temperature and decreasing soil moisture on global ecosystem
441 productivity using solar-induced chlorophyll fluorescence. Global Change Biology, 28(6),
442 2066–2080. https://doi.org/10.1111/gcb.16043

443 Drake JE, Tjoelker MG, Vårhammar A, Medlyn BE, Reich PB, Leigh A, Pfautsch S,
444 Blackman CJ, López R, Aspinwall MJ, Crous KY, Duursma RA, Kumarathunge D, De Kauwe
445 MG, Jiang M, Nicotra AB, Tissue DT, Choat B, Atkin OK, Barton CVM (2018) Trees tolerate
446 an extreme heatwave via sustained transpirational cooling and increased leaf thermal
447 tolerance. Glob Change Biol. 24: 2390–2402. https://doi.org/10.1111/gcb.14037

448 Forzieri, G., Dakos, V., McDowell, N.G. et al. (2022) Emerging signals of declining forest
449 resilience under climate change. Nature 608, 534–539. https://doi.org/10.1038/s41586-022-
450 04959-9

451 Fu, Z., Ciais, P., Prentice, I.C. et al. Atmospheric dryness reduces photosynthesis along a large
452 range of soil water deficits. Nat Commun 13, 989 (2022). https://doi.org/10.1038/s41467-022-
453 28652-7

454 Gessler, A., Bottero, A., Marshall, J. and Arend, M. (2020), The way back: recovery of trees
455 from drought and its implication for acclimation. New Phytol, 228: 1704-1709.
456 https://doi.org/10.1111/nph.16703

457 Getachew Mengistu, A., Mengistu Tsidu, G., Koren, G., Kooreman, M. L., Folkert Boersma, K.,
458 Tagesson, T., Ardö, J., Nouvellon, Y., & Peters, W. (2021). Sun-induced fluorescence and
459 near-infrared reflectance of vegetation track the seasonal dynamics of gross primary
460 production over Africa. Biogeosciences, 18(9), 2843-2857. https://doi.org/10.5194/bg-18-2843-
461 2021

https://doi.org/10.5194/egusphere-2024-423
Preprint. Discussion started: 26 February 2024

462 Gharun M., Vervoort R.W., Turnbull T.L., Adams M.A. (2014) A test of how coupling of
463 vegetation to the atmosphere and climate spatial variation affects water yield modelling in
464 mountainous catchments 514, pp. 202-213. https://doi.org/10.1016/j.jhydrol.2014.04.037

465 Gharun M., Hörtnagl L., Paul-Limoges E., Ghiasi S., Feigenwinter I., Burri S., Marquardt K.,
466 Etzold S., Zweifel R., Eugster W., Buchmann N (2020) Physiological response of Swiss
467 ecosystems to 2018 drought across plant types and elevationPhil. Trans. R. Soc.
468 B3752019052120190521. http://doi.org/10.1098/rstb.2019.0521

469 Gourlez de la Motte L, Beauclaire Q, Heinesch B, Cuntz M, Foltýnová L, Šigut L, Kowalska N,
470 Manca G, Ballarin IG, Vincke C, Roland M, Ibrom A, Lousteau D, Siebicke L, Neiryink J,
471 Longdoz B. (2020) Non-stomatal processes reduce gross primary productivity in temperate
472 forest ecosystems during severe edaphic drought. Philos Trans R Soc Lond B Biol Sci.
473 375(1810):20190527. doi: 10.1098/rstb.2019.0527.

474 Haesen, S., Lembrechts, J. J., De Frenne, P., Lenoir, J., Aalto, J., Ashcroft, M. B., Kopecký,
475 M., Luoto, M., Maclean, I., Nijs, I., Niittynen, P., van den Hoogen, J., Arriga, N., Brůna, J.,
476 Buchmann, N., Čiliak, M., Collalti, A., De Lombaerde, E., Descombes, P. … Van Meerbeek, K.
477 (2023). ForestClim—Bioclimatic variables for microclimate temperatures of European forests.
478 Global Change Biology, 29, 2886–2892. https://doi.org/10.1111/gcb.16678

479 Humphrey V, Zscheischler J, Ciais P, Gudmundsson L, Sitch S, Seneviratne SI. (2018)
480 Sensitivity of atmospheric CO2 growth rate to observed changes in terrestrial water storage.
481 Nature, 560 (7720): 628 DOI: 10.1038/s41586-018-0424-4.

482 Klein Tank, A. M. G., Wijngaard, J. B., Können, G. P., Böhm, R., Demarée, G., Gocheva, A.,
483 Mileta, M., Pashiardis, S., Hejkrlik, L., Kern-Hansen, C., Heino, R., Bessemoulin, P., Müller-
484 Westermeier, G., Tzanakou, M., Szalai, S., Pálsdóttir, T., Fitzgerald, D., Rubin, S., Capaldo,
485 M., … Petrovic, P. (2002). Daily dataset of 20th-century surface air temperature and
486 precipitation series for the European Climate Assessment. International Journal of Climatology,
487 22(12), 1441–1453. https://doi.org/10.1002/joc.773

488 Klein, T. (2014), The variability of stomatal sensitivity to leaf water potential across tree species
489 indicates a continuum between isohydric and anisohydric behaviours. Funct Ecol, 28: 1313-
490 1320. https://doi.org/10.1111/1365-2435.12289

https://doi.org/10.5194/egusphere-2024-423
Preprint. Discussion started: 26 February 2024

Li X et al. (2018) Solar-induced chlorophyll fluorescence is strongly correlated with terrestrial photosynthesis for a wide variety of biomes: first global analysis based on OCO-2 and flux tower observations Glob. Change Biol. 24 3990–4008.

Li, X., Xiao, J. (2019) A global, 0.05-degree product of solar-induced chlorophyll fluorescence derived from OCO-2, MODIS, and reanalysis data. *Remote Sensing*, *11*, 517; doi:10.3390/rs11050517.

Li, F., Xiao, J., Chen, J., Ballantyne, A., Jin, K., Li, B., Abraha, M., John, R. (2023) Global water use efficiency saturation due to increased vapor pressure deficit. Science, 381, 672-677. DOI: 10.1126/science.adf5041.

Magney T S et al. (2019) Mechanistic evidence for tracking the seasonality of photosynthesis with solar-induced fluorescence Proc. Natl Acad. Sci. USA 116 11640–5.

Marchin, R. M., Backes, D., Ossola, A., Leishman, M. R., Tjoelker, M. G., & Ellsworth, D. S. (2022). Extreme heat increases stomatal conductance and drought-induced mortality risk in vulnerable plant species. *Global Change Biology*, 28, 1133–1146. https://doi.org/10.1111/gcb.15976

Markonis, Y., Kumar, R., Hanel, M., Rakovec, O., Máca, P., AghaKouchak, A., (2021). The rise of compound warm-season droughts in Europe. Science Advances 7. https://doi.org/10.1126/sciadv.abb9668

McDowell, N. G. et al. (2020) Pervasive shifts in forest dynamics in a changing world. Science 368, eaaz9463.

Müller, L. M., and M. Bahn (2022) Drought legacies and ecosystem responses to subsequent drought. Global Change Biology 28:5086–103. doi:10.1111/gcb.16270.

Muñoz-Sabater, J., Dutra, E., Agustí-Panareda, A., Albergel, C., Arduini, G., Balsamo, G., Boussetta, S., Choulga, M., Harrigan, S., Hersbach, H., Martens, B., Miralles, D. G., Piles, M., Rodríguez-Fernández, N. J., Zsoter, E., Buontempo, C., & Thépaut, J. N. (2021). ERA5-Land: A state-of-the-art global reanalysis dataset for land applications. Earth System Science Data, 13(9), 4349–4383. https://doi.org/10.5194/essd-13-4349-2021

https://doi.org/10.5194/egusphere-2024-423
Preprint. Discussion started: 26 February 2024

Peters, W., van der Velde, I.R., van Schaik, E. et al. Increased water-use efficiency and reduced CO2 uptake by plants during droughts at a continental scale. Nature Geosci 11, 744–748 (2018). https://doi.org/10.1038/s41561-018-0212-7

Peters, R.L., Steppe, K., Pappas, C., Zweifel, R., Babst, F., Dietrich, L., von Arx, G., Poyatos, R., Fonti, M., Fonti, P., Grossiord, C., Gharun, M., Buchmann, N., Steger, D.N. and Kahmen, A. (2023), Daytime stomatal regulation in mature temperate trees prioritizes stem rehydration at night. New Phytol, 239: 533-546. https://doi.org/10.1111/nph.18964

Pickering, M., Cescatti, A., and Duveiller, G. (2022) Sun-induced fluorescence as a proxy for primary productivity across vegetation types and climates, Biogeosciences, 19, 4833–4864, https://doi.org/10.5194/bg-19-4833-2022.

Oren, R., Sperry, J.S., Katul, G.G., Pataki, D.E., Ewers, B.E., Phillips, N. and Schäfer, K.V.R. (1999), Survey and synthesis of intra- and interspecific variation in stomatal sensitivity to vapour pressure deficit. Plant, Cell & Environment, 22: 1515-1526. https://doi.org/10.1046/j.1365-3040.1999.00513.x

Röthlisberger, M., Papritz, L. (2023). Quantifying the physical processes leading to atmospheric hot extremes at a global scale. Nature Geosci. 16(3), 210-216. doi:10.1038/s41561-023-01126-1.

Seidl, R., Thom, D., Kautz, M. et al. Forest disturbances under climate change. Nature Clim Change 7, 395–402 (2017). https://doi.org/10.1038/nclimate3303

Seneviratne, S. I., Zhang, X., Adnan, M., Badi, W., Dereczynski, C., Di Luca, A., Ghosh, S., Iskandar, I., Kossin, J., Lewis, S., Otto, F., Pinto, I., Satoh, M., Vicente-Serrano, S. M., Wehner, M., and Zhou, B. (2021) Weather and Climate Extreme Events in a Changing Climate, in: Climate Change 2021: The Physical Science Basis. Contribution of Working Group I to the Sixth Assessment Report of the Intergovernmental Panel on Climate Change, edited by: Masson-Delmotte, V., Zhai, P., Pirani, A., Connors, S. L., Péan, C., Berger, S., Caud, N., Chen, Y., Goldfarb, L., Gomis, M. I., Huang, M., Leitzell, K., Lonnoy, E., Matthews, J. B. R., Maycock, T. K., Waterfield, T., Yelekçi, O., Yu, R., and Zhou, B., Cambridge University Press, Cambridge, United Kingdom and New York, NY, USA, 1513–1766, https://doi.org/10.1017/9781009157896.013.

https://doi.org/10.5194/egusphere-2024-423
Preprint. Discussion started: 26 February 2024

547 Shekhar, A., Hörtnagl, L., Buchmann, N., & Gharun, M. (2023a). Long-term changes in forest
548 response to extreme atmospheric dryness. Global Change Biology, 29, 5379–5396.
549 https://doi.org/10.1111/gcb.16846

550 Shekhar A, Hörtnagl L, Paul-Limoges E, Etzold S, Zweifel R, Buchmann N, Gharun M (2024)
551 Contrasting impact of extreme soil and atmospheric dryness on the functioning of trees and
552 forests. Science of the Total Environment 916, 169931.
553 https://doi.org/10.1016/j.scitotenv.2024.169931

554 Shekhar A, Buchmann N and Gharun M (2022) How well do recently reconstructed solar-induced
555 fluorescence datasets model gross primary productivity? Remote Sens. Environ. 283, 113282

556 Shekhar A, Humphrey V, Buchmann N, Gharun M (2023b). More than three-fold increase of
557 extreme dryness across Europe by end of 21st century. https://doi.org/10.21203/rs.3.rs-
558 3143908/v2 (under review in Weather and Climate Extremes)

559 Tripathy, K. P., & Mishra, A. K. (2023) How unusual is the 2022 European compound drought
560 and heatwave event? Geophysical Research Letters, 50, e2023GL105453.
561 https://doi.org/10.1029/2023GL105453

562 van der Woude, A.M., Peters, W., Joetzjer, E. *et al.* Temperature extremes of 2022 reduced
563 carbon uptake by forests in Europe. *Nat Commun* 14, 6218 (2023).
564 https://doi.org/10.1038/s41467-023-41851-0

565 van der Molen MK, Dolman AJ, Ciais P et al (2011) Drought and ecosystem carbon cycling.
566 Agric for Meteorol. 151(7):765–773. https://doi.org/10.1016/j.agrformet.2011.01.018

567 Zhang J, Xiao J, Tong X, Zhang J, Meng P, Li J, Liu P, Yu P (2022) NIRv and SIF better
568 estimate phenology than NDVI and EVI: Effects of spring and autumn phenology on ecosystem
569 production of planted forests. Agricultural and Forest Meteorology 315, 108819

570 Zhou, S., Yu, B. and Zhang, Y. (2023). Global concurrent climate extremes exacerbated by
571 anthropogenic climate change. Sci. Adv. 9(10), p.eabo1638. doi:10.1126/sciadv.abo1638.

572 Wang B, Chen T, Xu G, Wu G, Liu G (2023) Management can mitigate drought legacy effects
573 on the growth of a moisture-sensitive conifer tree species. Forest Ecology and Management
574 544, 121196. https://doi.org/10.1016/j.foreco.2023.121196